

Elastic properties and phase stability of AgBr under pressure.

P.T. Jochym* and K. Parlinski
*Institute of Nuclear Physics,
ul. Radzikowskiego 152, 31-342 Cracow, Poland*

Ab initio calculations have been used to derive the elastic constants, equation of state and free energy of NaCl, KOH and CsCl-type structures of AgBr. The elastic constants have been derived by the stress-strain relation. The shear elastic constants C_{44} has proved to be exceptionally soft. We have found that at temperature $T=0$ the phase transition from the low pressure NaCl-type to the high-pressure CsCl-type structure goes over a monoclinic KOH-type structure. The free energy comparison indicates that the monoclinic phase ranges from 8 to 35 GPa.

PACS numbers: 05.70.F, 64.60, 64.70, 71.15.Mb

Silver halide crystals are of considerable interest, since they exhibit deviation from the ideal ionic character due to the presence of the d-electrons in Ag^+ ions. Numerous studies of these crystals have been undertaken in the past years using various forms of interaction potentials including three-body interactions and van der Waals forces,^{1,2} as well as the *ab initio* total energy pseudopotential calculations.³ There are also many experimental works studying various aspects of these solids.^{4-7,10-13} The results of studies using phenomenological potentials generally show good agreement with experiment.² These studies use sophisticated schemes involving three body interactions and van der Waals potentials. The *ab initio* results for transition pressure seems to be less accurate³. There is one *ab initio* study of phase stability of silver bromide AgBr.¹⁴ Nevertheless, the transition mechanism is still unclear for this compound. Several models have been proposed,^{5-7,14-17} but the transition mechanism remains still an open problem. The *ab initio* study by Nunes, Allen and Martins,¹⁴ which investigated the energy of several candidate structures, proposed an intermediate trigonal phase with space group $P3_121$. In contrast recent experimental work of Hull and Keen¹⁵ suggested an existence of an intermediate phase with a monoclinic, KOH-type structure and shear instability as the transition mechanism. The silver bromide AgBr is stable at ambient temperature and pressure in the rocksalt structure $\text{Fm}\bar{3}\text{m}$. In ambient temperature and high pressures it has a second stable phase with CsCl structure $\text{Pm}\bar{3}\text{m}$. The phase transition in between these phases has been reported⁶⁻⁹ to occur at $P_t=8.3$ GPa. In this paper we are studying elastic properties and phase stability of the AgBr as a function of pressure. For NaCl and CsCl structures we have scanned pressures in the interval $P=0-200$ GPa, and calculated the free energies and elastic constants. In the range of $P=0-40$ GPa we have also studied the phase stability of the free, non-constrained by any symmetry, AgBr crystal, searching for any intermediate phases as well as general transition mechanism. The non-constrained crystal was treated as having $P1$ symmetry, however, its unit cell content was not allowed to change. Hence, phase transitions to phases with multiplication unit cells were not taken into account.

I. METHODOLOGY

The calculations have been performed using Density Functional Theory (DFT) approach with ultrasoft pseudopotentials and Generalised Gradient Approximation (GGA).¹⁸⁻²⁰ We have used CASTEP²¹ implementation of this method and pseudopotentials provided with this package. The elastic constants of the NaCl phase have been also verified by the independent calculation using VASP²². The electronic minimisation used density mixing scheme and pseudopotentials parametrised in the reciprocal space. The summation over the Brillouin zone has been performed with weighted summation over wave vectors generated by Monkhorst-Pack scheme.²³ All computations were done in $1\times 1\times 1$ supercell with 8 or 2 or 8 atoms for NaCl or CsCl or KOH structures, respectively. Some tests for NaCl has been carried out on the primitive, others on the face-centered cubic unit cell.

Due to high demands of the accuracy of the free energy, we have conducted extensive tests of convergence of the energy and pressure with respect to energy cutoff and Brillouin zone grid spacing parameters. Thus, we have performed a series of calculations with cutoff energies in the range of $E_{cut}=300-450$ eV and \mathbf{k} -space grid spacing in the range $\Delta\mathbf{k}=0.02-0.1 \text{ \AA}^{-1}$. In the light of obtained results we have decided to use in our computations a 0.4 \AA^{-1} grid spacing and 340 eV energy cutoff. The chosen grid corresponds to 32 wave-vectors for NaCl structure and 256 wave-vectors for CsCl structure. Such a large number of wave-vectors made calculations rather time-consuming. But since we are comparing energies of *different* structures with different unit cell volumes and Brillouin zone shapes, sizes and \mathbf{k} -sampling, we need a very good convergence of energy. At zero pressure the lattice constants of the optimised NaCl structure is $a=5.7859 \text{ \AA}$, while the experimental lattice constants at $P=0$ GPa and $T=300$ K is $A=5.7745 \text{ \AA}$.

II. FREE ENERGY AND EQUATION OF STATE

To investigate the phase stability of the crystal and to estimate the phase transition pressure, one must eval-

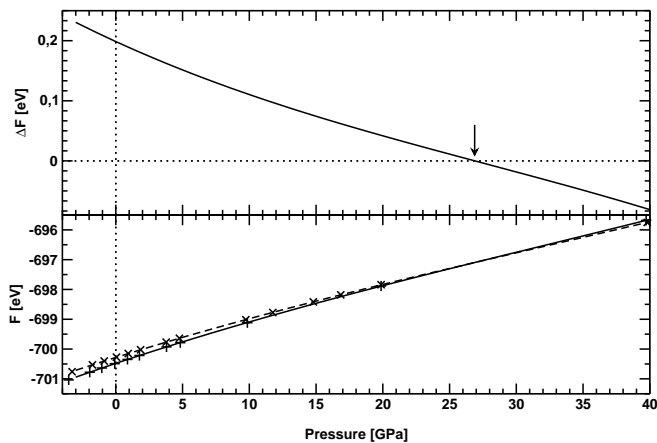


FIG. 1. Lower part: Free energy of AgBr in NaCl (+, solid line) and CsCl (x, dashed line) structures. Upper part: Free energy difference $F_{CsCl} - G_{NaCl}$ between CsCl and NaCl structures as a function of pressure. The vertical arrow denotes predicted phase transition pressure.

uate the free energy of all involved phases and choose the one with the lowest energy as stable. Since in *ab initio* calculations the temperature $T=0$, the free energy is: $F = E + PV$. We have performed calculations of the crystal free energy F for several pressures from 0 to 50 GPa for both NaCl and CsCl structures. Fig 1 shows the results of these computations. In the lower part the absolute values of free energies per atom are plotted together with cubic polynomials fitted to these data. In the upper part the difference of $F_{CsCl} - F_{NaCl}$ is plotted against pressure. The difference changes sign at the pressure $P_t=27$ GPa (arrow). We see that our calculations correctly predict that the rocksalt structure is more stable at low pressure and that at higher pressures the stability passes to CsCl structure. The large difference between experimental $P_t=8.3$ GPa and calculated $P_t=27$ GPa transition pressure could be attributed to a few factors. The main reason could be related to the appearance of the intermediate KOH-type structure, discussed below. Here, we mention other possible factors. First, the experimental data^{5,6} are measured only at ambient temperature, while the calculations were performed at $T=0$. At finite temperature the entropy contribution to the Gibbs free energy $G = E + PV - TS$ can also be different for the two structures, since the closest coordination shells contain different number of ions. Another reason could be related to the fact that the van der Waals interaction is neglected in DFT calculations, and that leads to under-binding of the crystal. This effect has already been noticed for silver iodide AgI crystal, where DFT predicts the phase transition pressure to be 10 GPa,^{2,3} while experimentally it is 4 GPa.

The data used to calculate free energy provide also the equation of state of the crystals. Fig. 2 shows the calculated equation of state for NaCl and CsCl structures as well as the experimental data measured by Bridgman and

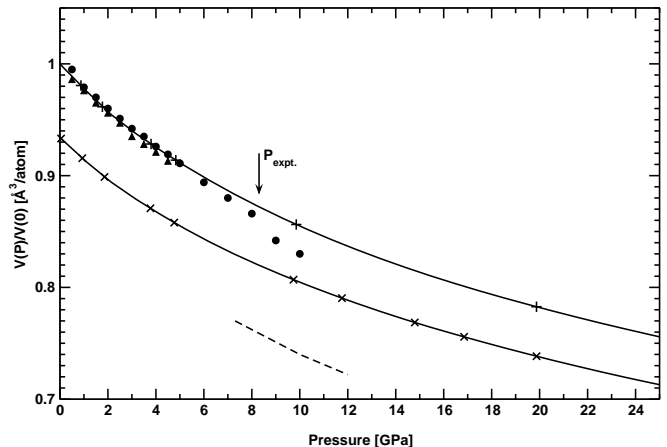


FIG. 2. Variation of relative volumes with pressure for NaCl(+) and CsCl (x) structure. Experimental points (●,▲) are taken from Bridgman^{5,6} and Vaidya¹⁰ respectively. The dashed line shows results of theoretical study of Gupta and Singh². The lines are present calculations.

Vaidya.^{5,6,10} We have also included in figure 2 the results of phenomenological study of Gupta and Singh.² This work was able to predict the transition pressure much better, but it fails to reproduce the volume compression of the phase transition. Present calculations show excellent agreement with experimental data for the low pressure range up to 6 GPa. In this interval the relative error in $V(P)/V(0)$ ratio is below 0.5%. It should be noted that the Bridgman measurements, are limited to 10 GPa and it would be interesting to increase the pressures to at least 15 GPa. We have also fitted the Murnaghan equation of state to rocksalt structure data below 15 GPa:

$$V = V_0 \exp \left[-\frac{\ln \left(\frac{PA_2}{A_1} + 1 \right)}{A_2} \right] \quad (1)$$

achieving good fit for $A_1=41.01$ GPa and $A_2=4.35$.

As seen from Fig. 2 the calculated relative volume change from NaCl to CsCl structure at the transition pressure $P_t=8.3$ GPa is a 6% compression. We are not aware of any experimental measurements of this value, however, we can estimate it from the Bridgman data⁶ to be at least 3%.

III. ELASTIC CONSTANTS

The behaviour of elastic properties of the AgBr is specially interesting in the vicinity of the phase transition. Fig. 3 shows pressure dependence of the bulk modulus as calculated from the equation of state, as well as from the following relationship with elastic constants:

$$B = -V \frac{\partial P(V)}{\partial V} = \frac{1}{3}(c_{11} + 2c_{12}) \quad (2)$$

The difference in the bulk modulus B between NaCl and CsCl structures is quite small. On the same figure 3

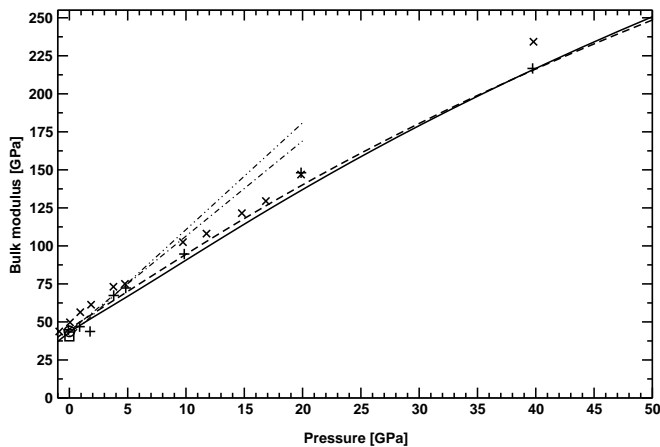


FIG. 3. Bulk modulus of AgBr calculated for NaCl structure from $P(V)$ function (solid line) and c_{ij} data (+) from Fig. 4. The bulk modulus for CsCl structure is calculated from $P(V)$ function (dashed line) and from c_{ij} data (\times) as well. Experimental data for $T=195$ K (\circ) and $T=300$ K (\square) are taken from Loje⁴. The dotted lines denote experimental pressure derivatives of B at zero pressure.

we have included two dotted lines showing experimental pressure derivatives of the bulk modulus at $P=0$ and $T=195$ K and $T=300$ K.⁴ From these data we see that our calculations reproduce the experimental bulk modulus quite well and that the results from different methods are consistent within 10%.

We have used the standard stress-strain relationship to derive all three elastic constants as a function of pressure. The method is based on constructing a set of linear equations from stress-strain relationships for several deformations of the unit cell. This set of equations represents a general form of the Hook's law and can be solved with respect to the elastic constants. Since in practice this set of equations is over-determined, to solve it we have used a singular value decomposition algorithm which automatically provides a least squares solution of the set²⁶. For each pressure three negative and three positive deformations of each kind, namely, bulk, shear and tetragonal elongation, have been set up.

Table I compares the calculated and experimental elastic constants at ambient pressure and two temperatures: $T=195$ K and $T=300$ K. Present results show quite good agreement with the measurements, although the calcu-

TABLE I. Experimental and calculated bulk modulus B and elastic constants c_{ij} of the AgBr crystal, in GPa. Values in parenthesis are calculated from $B = \frac{1}{3}(c_{11} + 2c_{12})$. Experimental data for $T=195$ K and $T=300$ K are taken from Loje⁴.

Result	B	c_{11}	c_{12}	c_{44}
Expt $T=300$ K	40.5	56.1	32.7	7.2
Expt $T=195$ K	43.81	63.13	34.14	7.65
Present	(44.84)	64.09	35.21	8.39
$B = -V\partial P(V)/\partial V$	42.56			

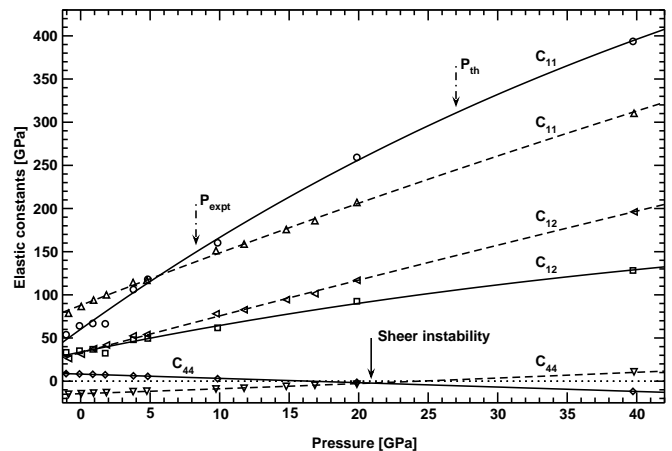


FIG. 4. Elastic constants c_{11} , c_{12} , c_{44} of AgBr in NaCl (solid lines and \circ , \square , \diamond) and CsCl (dashed lines and Δ , ∇) structures respectively. The lines are cubic fits to the calculation data. The vertical solid arrow denotes predicted shear instability pressure.

lations are performed at $T=0$. The temperature data points allow to extrapolate the experimental values to $T=0$. Thus, we have estimated that from $T=195$ K to $T=0$ K the elastic constants might increase by about 5%. The mechanism of the phase transition from NaCl to CsCl structure involves variation of the c_{44} elastic constant. We have calculated c_{44} for both NaCl and CsCl structures and for several pressures in the interval from 0 to 40 GPa. The results are shown at Fig. 4. We can clearly see that the two lines representing the c_{44} elastic constants, intersect at pressure $P=21$ GPa, and moreover at value close to zero. The pressure $P=21$ GPa of the shear instability and $P=27$ GPa of the free energy equality are not exactly the same. However, we shall see in the next section that in this pressure interval another phase could be more stable than the cubic NaCl or CsCl structures. In previous sections the calculation were performed for NaCl and CsCl structures under constrains

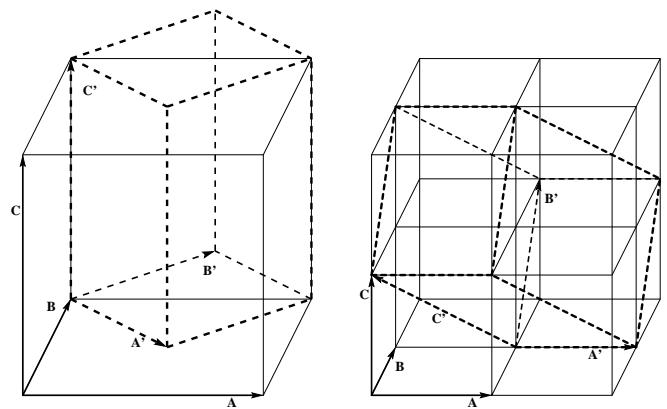


FIG. 5. Relation between cubic NaCl and monoclinic KOH (left) and between cubic CsCl and monoclinic KOH (right) unit cells. The KOH unit cell is drawn with dashed lines.

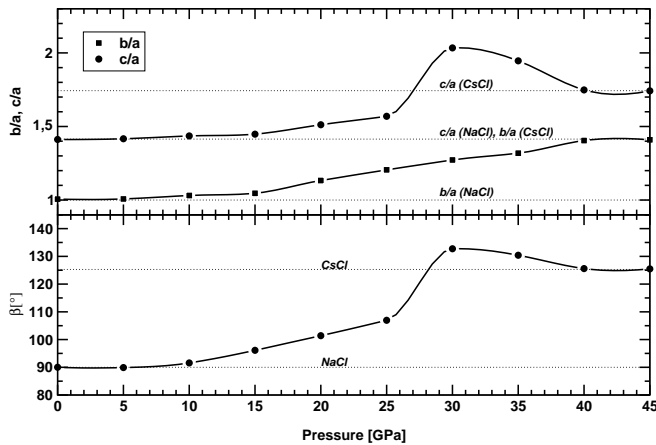


FIG. 6. Transition from NaCl to CsCl structure. Solid lines are guide to the eye.

that both phases remain always cubic. Now, we release this restrictions and allow the unit cell to deform to a structure of P1 symmetry being intermediate configuration between the NaCl and CsCl ones.

IV. INTERMEDIATE PHASE

When the intermediate configuration becomes monoclinic it resembles the KOH-type structure. The relationship between NaCl, KOH and CsCl structures is shown on Fig.5. Setting the monoclinic angle $\beta=90^\circ$ or $\beta=125.27^\circ$ one reestablishes the NaCl or CsCl structures, respectively. Hull and Keen¹⁵ pointed out that this monoclinic phase, may provide a proper transition path between NaCl and CsCl structures. A detailed study of the above phase transition mechanism has been performed and we refer the results below. We have prepared a model of the AgBr crystal in the KOH-type structure

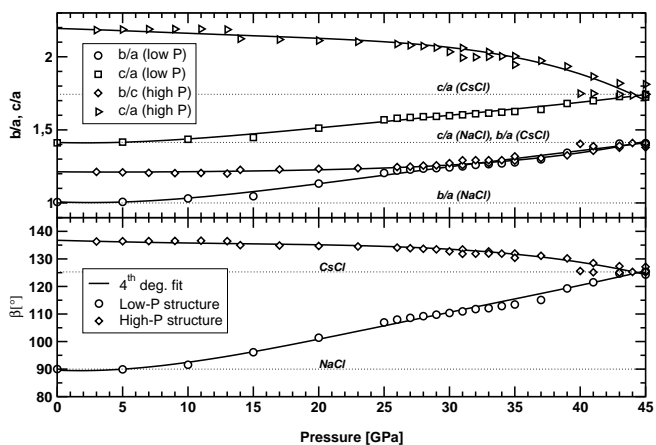


FIG. 7. Cell parameters in NaCl structure to CsCl structure transition of AgBr. Solid lines are fourth degree fits to the data points.

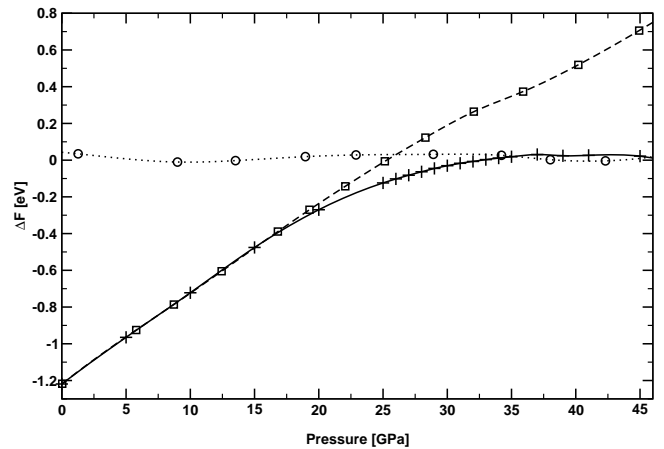


FIG. 8. Free energy difference in the transition of AgBr from NaCl (squares) to CsCl structure (circles) through KOH structure (crosses). The polynomial fit to the CsCl data points is taken as the reference line (zero level). The lines are guide to the eye.

with cell volume corresponding to the NaCl structure at $P=0$. The β angle of the monoclinic unit cell was set to 110° . Then the crystal geometry inducing atomic relaxations was optimised with respect to free energy for various increasing pressures from 0 to 45 GPa. At each pressure the minimisation procedure was reiterated several times since large changes in the unit cell size involved changes of the Brillouin zone grid. The results are plotted in Fig 6. One notices that at about 8 GPa, there is a clear tendency to depart from the pure NaCl structure to an intermediate monoclinic structure. There is also a clear jump of lattice parameters at the $P=25\text{--}30$ GPa range. Simultaneously, the α , and γ angles do not change by more than 0.05° for the scanned pressure range. To verify the last findings we have carried out two series of calculations each starting from the same either low or high pressure configurations. The starting low and high pressure configurations were taken from optimised monoclinic configurations at $P_{lo}=25$ GPa or $P_{hi}=30$ GPa, respectively. The results are shown in Fig. 7. It is clear from this figure that both monoclinic structures may show weak metastable behaviour. However, the energy difference is small and it is possible that this effect will manifest itself only in low temperatures. Furthermore, the energy of the high-pressure configuration is always above the low-pressure one. Consequently, the high-pressure structure is probably never present in the real crystal, and we will omit this structure from now

TABLE II. Calculated elastic constants (in GPa) of the monoclinic, KOH-type structure of the AgBr under pressure of $P=20$ GPa.

Pressure [GPa]	c_{11}	c_{22}	c_{33}	c_{12}	c_{13}	c_{23}
20	156	175	229	152	84	98

TABLE III. Calculated structural parameters of the intermediate KOH-type structure of the AgBr crystal.

P [GPa]	a [Å]	b [Å]	c [Å]	β [°]	b/a	c/a
0	4.0803	4.1064	5.7601	90.0	1.006	1.412
5	3.9521	3.9819	5.5982	89.9	1.008	1.417
10	3.8226	3.9411	5.4886	91.6	1.031	1.436
15	3.7368	3.9091	5.4100	96.1	1.046	1.448
20	3.5445	4.0156	5.3589	101.4	1.133	1.512
25	3.4033	4.1011	5.3403	107.0	1.205	1.569
30	3.2993	4.1976	6.7106	132.7	1.272	2.034
35	3.2316	4.2612	6.2892	130.4	1.319	1.946
40	3.1725	4.4554	5.5465	125.6	1.404	1.748
45	3.1489	4.4375	5.4855	125.5	1.409	1.742

on. Difference of the free energy of the three optimised candidate structures (NaCl, KOH, CsCl) are shown in Fig. 8. The polynomial fit to the CsCl free energy data is taken as the reference line (“0” level). At zero pressure the NaCl structure is the most stable one. When we increase the pressure above about 8 GPa, the cubic symmetry is broken, the monoclinic angle β starts to increase and the monoclinic phase is favoured. At the special point at $P=21$ GPa, at which the shear elastic constants c_{44} of NaCl and CsCl structure vanish on the Fig. 4, the monoclinic phase is still the most stable one. Only above $P=35$ GPa the CsCl structure becomes the most stable phase. However, for the finite temperature case this might change, since the NaCl and CsCl structures have different number of atoms in coordination shells and hence different entropy terms in the Gibbs free energies. Since there are no low temperature measurements of pressure dependent behaviour of the AgBr we cannot compare the present results with experimental findings.

We have also, for completeness, calculated some elastic constants of the intermediate KOH phase of the crystal. The monoclinic phase has 13 independent elastic constants. However, due to the small energy difference between phases connected by the shear deformation, only 6 of them can be calculated accurately. The remaining 7 constants are too small and could be only estimated to be below 10 GPa. This is quite expected result. The 6 large elastic constants, calculated under pressure of $P=20$ GPa are presented in the Table II. The values are consistent with the values of elastic constants of NaCl and CsCl structures depicted on the Fig. 4.

Summarising, our results support the hypothesis formulated by Hull and Keen,¹⁵ that the phase transition from NaCl to CsCl phase, goes through the intermediate KOH-type, monoclinic structure.

V. CONCLUSIONS

The present DFT calculations show that at temperature $T=0$ K the cubic NaCl and CsCl-type structures of AgBr are stable at pressures 0–8 GPa and above 35 GPa,

respectively. Moreover, the calculation performed in constraints of these two cubic structures permit to find the equation of state and the elastic constants in the whole interesting range of pressures from 0 to 45 GPa. It is interesting to see that the shear elastic constants c_{44} for both phases NaCl and CsCl vanish close to 21 GPa. The derived equation of state and the elastic constants characterise properly the stable cubic phase, and additionally can provide a useful estimation of similar quantities within the intermediate monoclinic phase. The calculation of the elastic constants of the monoclinic KOH phase showed that, due to the small energy difference between phases, the KOH phase is very soft to shear deformations and its elastic constants are consistent with the elastic constants of the other two phases.

The study of the intermediate phase has been done without point symmetry elements constraints. This means that any deformation of the simulated supercell could have taken place. The only imposed limitation was the number of atoms in the supercell. Due to this approach the supercell remained always monoclinic (or cubic for special values of monoclinic angle β). The values of the free energy of the three candidate phases indicate that the monoclinic phase becomes the most stable one in the pressure interval from 8 to 35 GPa. This structure has previously been proposed to be the transformation path between NaCl and CsCl-type phases. And indeed, the free energy of the intermediate monoclinic phase seems to be lower than these of the cubic ones. However the difference in energy is quite small, which means that defects and impurities present in the crystal could show a large impact on the monoclinic phase.

ACKNOWLEDGMENTS

The use of facilities of the ACC “Cyfronet”, Cracow, where the calculations have been done, are kindly acknowledged. This work was partially supported by the Polish State Committee of Scientific Research (KBN), grant No 2 PO3B 004 14, and computational grant No. KBN/SGLORIGIN_2000/IFJ/128/1998.

-
- * Pawel.Jochym@ifj.edu.pl
- ¹ R.K. Singh, P. Khare, *phys. stat. sol. (b)* **103**, 337 (1981)
 - ² D.C. Gupta and R.K. Singh, *Phys. Rev. B*, **43** 11185 (1991).
 - ³ J.R. Chelikowsky, *Phys. Rev. B* **35**, 1174 (1987)
 - ⁴ K.F. Loje and D.E. Schuele, *J. Phys. Chem. Solids*, **31** 2051 (1970).
 - ⁵ P.W. Bridgman, *Proc. Am. Acad. Arts Sci.*, **74**, 21 (1940)
 - ⁶ P.W. Bridgman, *Proc. Am. Acad. Arts Sci.*, **76**, 1 (1945)
 - ⁷ T.E. Slykhouse and H.G. Drickamer, *J. Phys. Chem. Solids* **7**, 207 (1958)
 - ⁸ W.A. Bassett and T. Takahashi, *Am. Mineral.* **50**, 1576 (1965)
 - ⁹ B.M. Riggleman and H.G. Drickamer, *J. Chem. Phys.* **38**, 2721 (1963)
 - ¹⁰ S.N. Vaidya and G.C. Kennedy, *J. Phys. Chem. Solids*, **32** 951 (1971)
 - ¹¹ T.A. Fjeldly and R.C. Hanson, *Phys. Rev. B* **10** 3569 (1974)
 - ¹² B.E. Mellander, *Phys. Rev. B* **26** 5886 (1982)
 - ¹³ S. Ves, D. Glötzel, M. Cardona and H. Overhof, *Phys. Rev. B* **24** 3073 (1981)
 - ¹⁴ G.S. Nunes, P.B. Allen, J.L. Martins, *Phys. Rev. B* **57**, 5098 (1998)
 - ¹⁵ S. Hull, D.A. Keen, *Phys. Rev. B* **59**, 750 (1999)
 - ¹⁶ K. Kusaba, Y. Syono, T. Kikegawa, O. Shimomura, *J. Phys. Chem. Solids* **56**, 751 (1995)
 - ¹⁷ R.N. Schock and J.C. Jamieson, *J. Phys. Chem. Solids* **30**, 1527 (1969)
 - ¹⁸ J.S. Lin, A. Qteish, M.C. Payne and V. Heine, *Phys. Rev. B* **47**, 4174 (1993).
 - ¹⁹ J. Goniakowski, J.M. Holender, L.N. Kantorovich, M.J. Gillan and J.A. White, *Phys. Rev. B* **53**, 957 (1996).
 - ²⁰ M.C. Payne, M.P. Teter, D.C. Allan, T.A. Arias, J.D. Joannopoulos, *Rev. of Mod. Phys.* **64**, 1045 (1992)
 - ²¹ CASTEP is a part of *Cerius²* system developed by Molecular Simulations.
 - ²² G. Kresse and J. Furthmüller, VASP program, Vienna (1999); *Phys. Rev. B* **54**, 11169 (1996); *Comput. Mat. Science* **6**, 15 (1996).
 - ²³ H.J. Monkhorst and J.D. Pack, *Phys. Rev. B* **13**, 5188 (1976).
 - ²⁴ S. Froyen, M.L. Cohen, *J. of Phys. C: Solid State Physics*, **19**, 2623 (1986).
 - ²⁵ S. Froyen, M.L. Cohen, *Phys. Rev.* **29**, 3770 (1984).
 - ²⁶ W. H. Press, B.P. Flannery, S.A. Teukolsky, and W.T. Vetterling, *Numerical Recipes* (Cambridge Univ. Press, 1988), p.301